J Electroceram (2007) 18:121–128
DOI 10.1007/s10832-007-9014-9

La_2O_3–B_2O_3–TiO_2 Glass/BaO–Nd_2O_3–TiO_2 ceramic for high quality factor low temperature co-fired ceramic dielectric

Seong-Jin Hwang · Yu-Jin Kim · Hyung-Sun Kim

Received: 11 February 2006 / Accepted: 5 October 2006 / Published online: 9 February 2007

Abstract A conventional BaO–Nd_2O_3–TiO_2 ceramic of microwave dielectric material was added to rare-earth derived borate glasses (La_2O_3–B_2O_3–TiO_2) for use as LTCC (low temperature co-fired ceramic) materials. The sintering behavior, phase evaluation, and microwave dielectric properties were investigated. It was found that increasing the sintering temperature from 750 to 850 °C led to increases in shrinkage and microwave dielectric properties (≈15 for ε_r , >10,000 GHz for Q^*f_0 and >94 ppm/ °C for τ_f at 7–8 GHz for resonant frequency). The results suggest that a composite with suitable additives for τ_f could feasibly be developed as a material for LTCC applications.

Keywords LTCC · Glass-ceramic · Microwave properties · Surface crystallization

1 Introduction

Microwave dielectric materials have been used for wireless applications and have also been developed for practical use in microwave filters, resonators, and mobile communication technology. To further increase the volume efficiency of microwave devices in communication systems, multilayer structures have been developed [1–4]. It is imperative to lower the sintering temperature of dielectric ceramics (<900 °C) in order to co-fire with a high conductivity electrode such as silver and palladium in multilayer structures. Low temperature co-fired ceramic (LTCC) technology provides a viable solution to these challenges [2–9]. LTCC materials for microwave applications require microwave dielectric properties, such as high dielectric constant (ε_r), high quality factor (Q^*f_0), and a small temperature coefficient of resonant frequency (τ_f) [5–10].

In LTCC technology, three methods have been commonly applied in reducing the sintering temperature of the dielectric: addition of low melting temperature glass [2–4], chemical processing [5], and use of smaller size particles for starting materials [6]. Among these processes, adding a low melting glass into a ceramic having excellent microwave properties has been the most favored process. Low melting glasses such as B_2O_3–ZnO glass and B_2O_3–BaO–SiO_2 glass have been considered based on several attributes related to sintering temperature, viscosity, solubility, and wetting behavior to form co-fired ceramics [2–4]. However, all glasses possess a low microwave dielectric quality factor because of the dispersing nature of microwaves [7, 8]. Conduction, ionic relaxation, deformation, and vibration loss in glasses have been the main obstacles to the use of these materials in the range of high frequency.

If glass is converted to glass-ceramics after forming crystal phases, the dielectric loss would be reduced. In order to mitigate the low quality factor in the microwave dielectric, low melting temperature glass has to be transformed into optimized crystallization having low dielectric loss during sintering process [9–14]. Previous research on glass-ceramics has led to the development of three leading methods of optimizing crystallization. One method involves the addition of metal oxides such as TiO_2 and Al_2O_3 into the glasses [10]. The second method employs a mixture of glass (50∼60 wt.%) and ceramic (50∼40 wt.%) [11–14] while the third deals only with a glass system based on crystalline kinetics and mechanism [15]. However, glass-ceramic materials must be considered in conjunction with the sintering conditions related to densification and crystal-

S.-J. Hwang · Y.-J. Kim · H.-S. Kim (✉)
School of Materials Engineering, Inha University,
253 Younghyun-dong, Nam-gu, Incheon 402-751, South Korea
e-mail: kimhs@inha.ac.kr

lization. In order to obtain a greater amount of crystallization in a glass-ceramic, we adopted the second method with 80 wt.% glass composition and 20 wt.% ceramic.

The aim of this paper is to demonstrate that it is possible to transform a glass having a low quality factor into a glass-ceramic possessing excellent microwave properties. The transformation of the glass (80 wt.% glass composition and 20 wt.% ceramic) into a glass-ceramic must proceed through a process of complete densification as well as appropriate crystallization. A rare earth derived glass composition (La_2O_3–B_2O_3–TiO_2) was used for the low melting glass composition, because of the low viscosity of the glass composition, high dielectric constant, and optimized crystallization. A commercial BNT (BaO–Nd_2O_3–TiO_2) ceramic with good microwave dielectric properties (≈90 for ε_r, ≈6000 GHz for $Q*f_0$, and 6.24 ppm/°C for τ_f) was used for the microwave ceramic [11–14]. The product obtained through this process can be used for low temperature co-fired ceramic materials for microwave applications.

2 Experimental procedure

The raw materials for the glass frit were La_2O_3, H_3BO_3, and TiO_2, which have high purity (Aldrich, USA). The batch G ($20La_2O_3$–$60B_2O_3$–$20TiO_2$ (in mol%)) was melted in a platinum crucible at 1,300 °C for 1 h. The glass melt was quickly poured and quenched on a copper plate and pulverized in a planetary mill for 10 h (mean diameter: 1.5 μm). For the preparation of bulk specimens, melts from a furnace were poured into a metal mould and heated to a temperature of 10 °C above the glass transition temperature (Tg=657 °C). The mould was then moved back into the furnace to anneal the glass for 1 h, and was then cooled very slowly in the furnace.

The ceramic material used was a commercial BNT (BaO–Nd_2O_3–TiO_2) ceramic powder (MBRT90, Fuji Titanium Ind. Japan, d_{50}: 2.9 μm), which was determined via XRD (X-ray diffractometer, APD system, PANalytical, Almero, Netherlands) to be thermally stable in the single $BaNd_2Ti_5O_{14}$ phase. The glass powder (80–30 wt.%) and ceramic materials (20–70 wt.%) were mixed using a ball mill for 24 h and then dried. The dried powder was formed pellets using a metal mould (1.5 cm in diameter and 0.8 cm in height). The G glass/BNT ceramic composites is presented in Table 1. To improve the densification, cold isostatic pressing (under 200 MPa) was applied to the pellets, which were sintered in a temperature range of 750∼850 °C for 1 h at a heating rate of 10 °C/min.

Table 1 Composition of G glass/BNT ceramic composites (in wt.%).

Composition	C1	C2	C3	C4	C5	C6
G (LBT glass)	80	70	60	50	40	30
BNT ceramic	20	30	40	50	60	70

The bulk density of the sintered samples was determined by the Archimedes method. The glass transition temperature (Tg) and the crystallization peak (Tp) were determined using a differential thermal analyzer (DTA-TA 1600, TA instruments, New Castle, DE) at a heating rate of 10 °C/min. Glass fibers of 0.5∼0.75 mm diameter and 23.5 cm length were made for testing Ts (Littleton softening point). This is the point at which the rod elongates under its own weight at a rate of 1 mm/min. The shrinkage of the samples was measured by a dilatometer (Model DIL402 PC, Netzsch Instruments, Selb, Germany). The microstructure of the samples was examined using a scanning electron microscopy (SEM) and an Energy Dispersive X-Ray Microanalysis System (EDAX, HITACHI, Tokyo, Japan). The crystal phase of the samples was detected using XRD (X-ray diffractometer, APD system, PANalytical, Almero, Netherlands). Microwave dielectric properties were measured on a network analyzer (8720Es, Agilent, Palo Alto, CA) at a range of 4–8 GHz using a resonant cavity and a split-post test fixture. The temperature coefficient of resonant frequency was measured as over a range of 25–120 °C [16–18].

3 Results and discussion

Using a DTA, the glass transition temperature (Tg: 657 °C) of the glasses was found to be at the same temperature for different glass frit sizes (Table 2). It was found that the onset point of crystallization (Tc) and crystallization temperature (Tp) increased with an increase of the frit size (1.5 μm<6 μm<45 μm<bulk). The effect of frit size on the Tg and Tp of the glass suggests that the crystallization of the G glass occurred from the surface rather than from the bulk. The Littleton softening point (Ts, $\eta=10^{7.6}$ dPa) of G glass was found at 722 °C. In view of the glass properties, such as

Table 2 Thermal properties of glass (frit and bulk).

Temperature(°C)	G ($20La_2O_3$–$60B_2O_3$–$20TiO_2$ glass in mol%)			
	Frits size (d_{50} :μm)			
	1.5	6	45	Bulk
Tg	657	657	657	657
Ts	722	722	722	722
Tc	778	785	801	835
Tp	798	809	815	899
Tm	1,043			

Tg: Glass transition temperature, *Ts*: Littleton softening point, *Tc*: onset point of crystallization, *Tp*: crystallization peak temperature, *Tm*: melting temperature.

Tg and Ts, the G glass appeared to be suitable to enhance the sinterability of the composites (glass and ceramic). It is believed that the G glass can be sintered as a matrix at the required temperature, which is lower than 900 °C.

The starting temperature of shrinkage was remarkably different for the BNT ceramic and for the composites, as shown in Fig. 1. The shrinkage of the BNT ceramic started at 1,210 °C, while the composites mixed with BNT ceramic and G glass frit shrank at a temperature of 710 °C. Above the Littleton softening point of the glass (Ts=722 °C), the shrinkage of composites dramatically increased and different maximum shrinkage was reached depending upon the mixture ratio in the composites. The finishing (complete) temperature for shrinkage in Fig. 1 shifted slightly to higher temperature with increasing ceramic content in the composites. The shrinkage of C1 composite was the highest (≈25%) in all composites. With a lower content of ceramic, higher shrinkage was found in the glass-ceramic composites.

The DTA results in Table 3 suggest that the composites with lower content of glass frit crystallized at lower temperature. Comparison of the thermal properties of the glass with those of the composites (C1–C6) reveals a slight decrease in the Tc (onset point of crystallization) and Tp (peak point of crystallization) with decreasing glass frit content in the composites. The effect of the relative amount of frit and ceramic on Tc and Tp is attributed to the faster formation of a crystal phase between the G glass and BNT ceramic with C3∼C6 composites than with C1 and C2. However, a detailed explanation of the crystallization mechanism is beyond the scope of this work.

The degree of densification is shown by the relative density of the composites (Fig. 2). The relative density of the composite increased up to approximately 90% with a gradually increasing amount of G glass frit. The highest value of relative density (>85%) appeared in composites of C1 and C2. As indicated by the DTA results in Table 2, the formation of a crystal phase in C1 and C2 composites occurred late relative to other composites. In view of the DTA results and the relative density, the C1 and C2 composites are anticipated to crystallize with a higher shrinkage rate and longer crystallization time. For this reason, C1 and C2, which display a relatively high dense microstructure, were chosen as the appropriate composition for closes study.

Table 3 DTA results of G and composites (heating rate: 10 °C/min).

Temperature (°C)	G glass and composites						
	G glass (1.5 μm)	C1	C2	C3	C4	C5	C6
Tc	778	766	760	759	758	755	754
Tp	798	787	785	775	769	766	764
Δ(Tp−Tc)	20	21	25	16	11	11	10

Tp Peak temperature of crystallization, *Tc* onset point of crystallization.

As shown in Fig. 3, the sintered composites of C1 and C2 included irregular pores generated by sintering and crystallization. The porosity of the C1 composite sintered with increasing temperature decreased, accompanied by lowering of pore size. However, the porosity and pore size of C2 sintered with increasing temperature showed an increasing trend. This variation in the porosities of C1 and C2 appears to be due to a difference in the starting temperature for densification and crystallization (Fig. 2 and Table 3). Thus, ceramic fillers (BNT ceramic) that are added to the glass matrix play a role of nuclei for crystallization of the glass matrix. Furthermore, the dissolution of ceramic filler into the glass matrix changes the composition of the glass and the starting temperature of crystallization. The degree of composition change depends

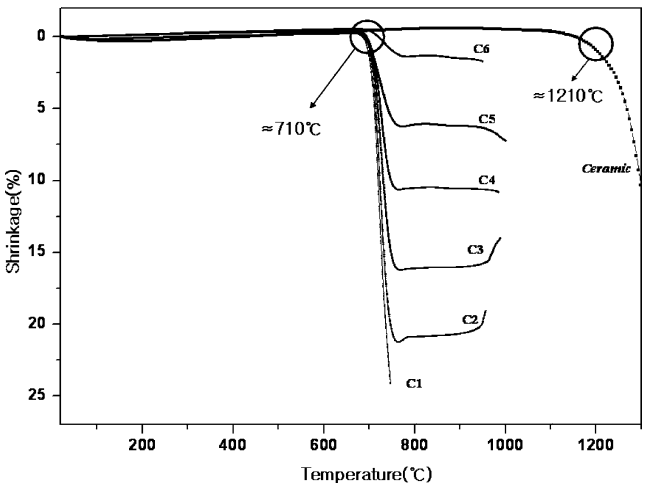

Fig. 1 Shrinkage of the composites and ceramic with increasing temperature (heating rate: 10 °C/min)

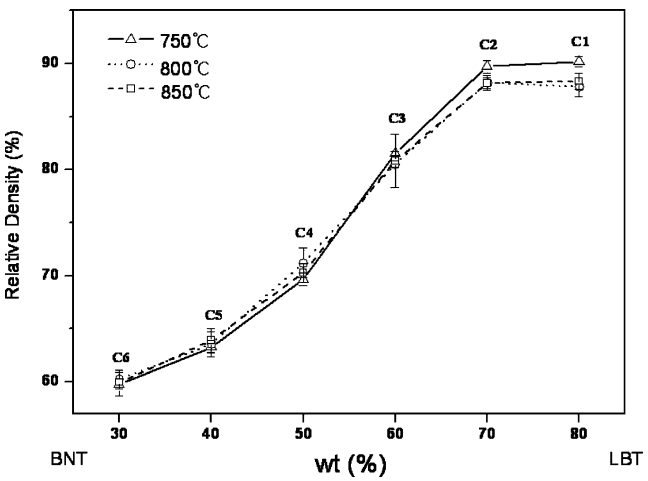

Fig. 2 Relative theoretical density of the G glass/BNT ceramic composites, where LBT and BNT denote glass (La_2O_3–B_2O_3–TiO_2) and ceramic powder (BaO–Nd_2O_3–TiO_2), respectively

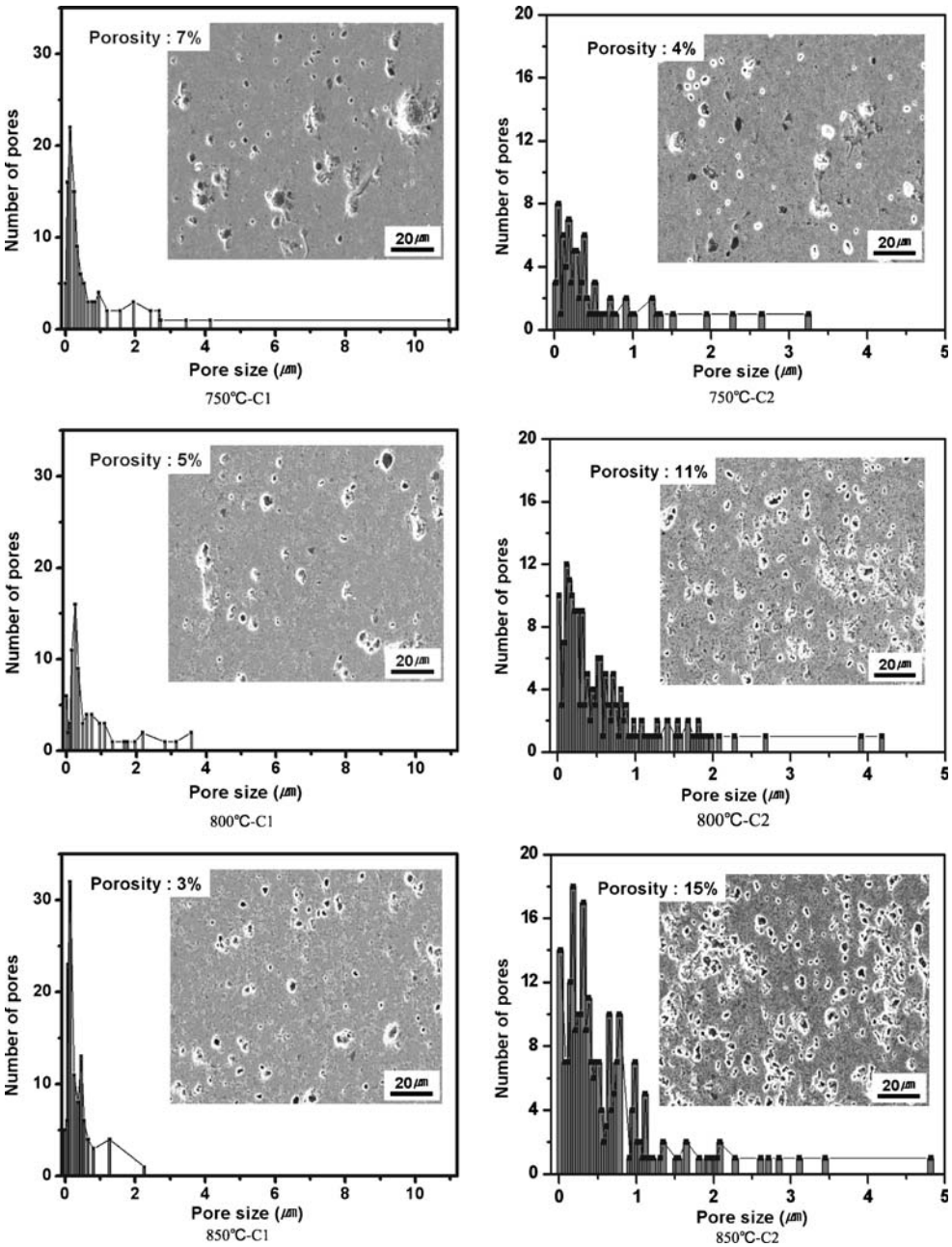

Fig. 3 Distribution of pore size and morphologies of composites (C1 and C2) as a function of firing temperature

on the ratio of the glass to the ceramic filler. Therefore, C1 and C2 have a different crystallization starting temperature.

The crystal phases of C1 and C2 composites sintered at the firing temperature, the G glass frit fired at 750~850 °C, and the BNT ceramic powder were identified from JCPDS cards, as shown in Fig. 4. Only G glass sintered above 750 °C was completely decomposed in the crystal phases of LaB_3O_6 and TiO_2, as given by relation (1).

$$(La_2O_3-3B_2O_3-TiO_2)_{glass} \xrightarrow{>750^{\circ}C} 2LaB_3O_{6(s)}+TiO_{2(s)} \quad (1)$$

However, the crystal phases of composites sintered as a function of temperature are new crystal phases of $LaBO_3$–LT, HT (JCPDS No. 72-0074, 76-0316), and the crystal phases of LaB_3O_6 (JCPDS No. 73-1150) and TiO_2 (JCPDS No. 76-0316) produced from the G glass follow relation (2–3).

$$(La_2O_3-3B_2O_3-TiO_2)_{glass}+(BaO-Nd_2O_3-TiO_2)_{ceramic} \xrightarrow{750^{\circ}C} LaB_3O_{6(s)}+TiO_{2(s)}+(LaBO_3-LT)_{(s)}+\text{residual glass} \quad (2)$$

$$(La_2O_3-3B_2O_3-TiO_2)_{glass}+(BaO-Nd_2O_3-TiO_2)_{ceramic} \xrightarrow{>800^{\circ}C} LaB_3O_{6(s)}+TiO_{2(s)}+(LaBO_3-HT)_{(s)} \quad (3)$$

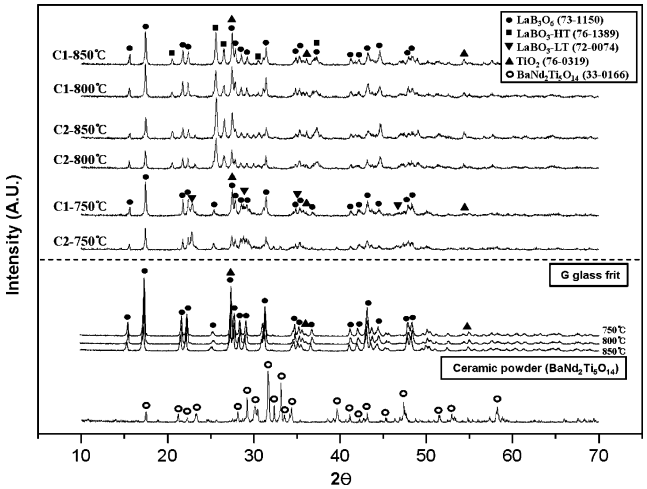

Fig. 4 X-ray diffraction patterns showing different phases of the materials and the sintering temperature. *LT* low temperature, *HT* high temperature

This implies that a certain amount of G glass transforms to the crystal phase of LaB_3O_6 and TiO_2, as suggested by a previous work [9]. However, comparing the C1 and C2 composites sintered above 800 °C, the main crystal phase was dependent upon the content of BNT ceramic. It is deduced that as the amount of BNT ceramic is increased, more $LaBO_3$ crystal phase will be generated. Thus, the crystal phase of $LaBO_3$ would be produced by the reaction between the G glass and BNT ceramic. In addition, the crystal phase of $LaBO_3$ is divided into two classes, $LaBO_3$–LT and $LaBO_3$–HT, according to the sintering temperature following chemical Eq. 4.

$$(LaBO_3-LT)_{(s)} \overset{>800^{\circ}C}{\longrightarrow} (LaBO_3-HT)_{(s)} \quad (4)$$

Consequently, the BNT ceramic dissolved into the G glass is thought to be a solid solution. This result is also related to the EDX analysis results (Table 4). The high resolution SEM image visually shows the three different regions delineated in the EDX analysis (Fig. 5 and Table 4). According to the XRD results, there are three crystal phases, LaB_3O_6, $LaBO_3$–HT, and TiO_2, in the C1 composite sintered at 850 °C. Based on the EDX and XRD results, the three regions (white, grey, and black) are $LaBO_3$–HT solid solution; Ba, Ti, and Nd for white, LaB_3O_6 for grey, and TiO_2 for black.

Based on the XRD and EDX results, the schematic diagram in Fig. 6 explains the crystallization of the composite without considering the shape of phase and porosity. In the sample sintered at 750 °C, there are four crystal phases: LaB_3O_6, TiO_2, $LaBO_3$–LT, and the residual glass. The four crystal phases are formed by G glass and G glass dissolved BNT ceramic at each region. However, at temperatures higher than 800 °C, the residual G glass changes to LaB_3O_6, TiO_2, and $LaBO_3$–HT, which is generated by a reaction between G glass and BNT ceramic. Furthermore, $LaBO_3$–LT formed at 750 °C is converted to $LaBO_3$–HT. After the final crystal phases are formed, they follow the process of grain growth with increasing sintering temperature.

The network analysis results indicate that the dielectric constants of C1 and C2 composites sintered as a function of temperature increased with decreasing resonant frequency (Table 5). The quality factor (Q^*f_0) was measured with C1 that was sintered as a function of temperature, C2 sintered at 800 °C, and BNT ceramic sintered at 1,280 °C. The measurement results indicate that the microstructure of the sintered samples is closely related to the quality factor [19]. The quality factors of sintered C1 increase with an increase in sintering temperature. As noted earlier, the relative density (>90%) and porosity (>3%) of the sintered samples, which reflect high densification, lead to a high quality factor.

As the sintered glass is composed of a number of pores generated by surface crystallization, the dielectric constant and other properties of the samples were not evaluated. On the other hand, the temperature coefficient of resonant frequency and the quality factor in C2 were determined for a sample sintered at 800 °C, which has a relatively low porosity. As suggested in Table 5, G glass and BNT ceramic have approximately 4 GHz of resonant frequency, while C1 and C2 composites possess about 7.5 GHz of resonant frequency. The dielectric constant for composites (C1 and C2) was about 13–16 at high frequency (7–8 GHz). Based on a mixture rule using various theories to predict the dielectric constants of materials, the dielectric constant of the composites was found to be 12∼24 [20]. Prediction of the dielectric constants is considered on the basis of phases, shape of phases, and porosity [19]. However, in this work, it was difficult to predict the dielectric constants of C1 and C2 composites that were sintered as a function of temperature because of the crystallization.

The temperature coefficient of resonant frequency is completely dependent upon the crystal phases. Comparing the C1 specimen sintered at 750 °C with the C1 specimen

Table 4 EDX analyses for regions in Fig. 5.

Elements	B*	O	Ti	La(Ba)*	Nd	Bi	Total
White (W)[a]	–	62.6	10.9	20.9	5.1	0.5	100
Grey (G)	–	74.2	–	25.8	–	–	100
Black (B)	–	67.6	23.9	5.7	2.3	0.5	100

[a] Mark of regions in Fig. 5.
* Boron was not detected because of the sensitivity of the instrument, and barium was not included because of its low content and similarity with lanthanum.

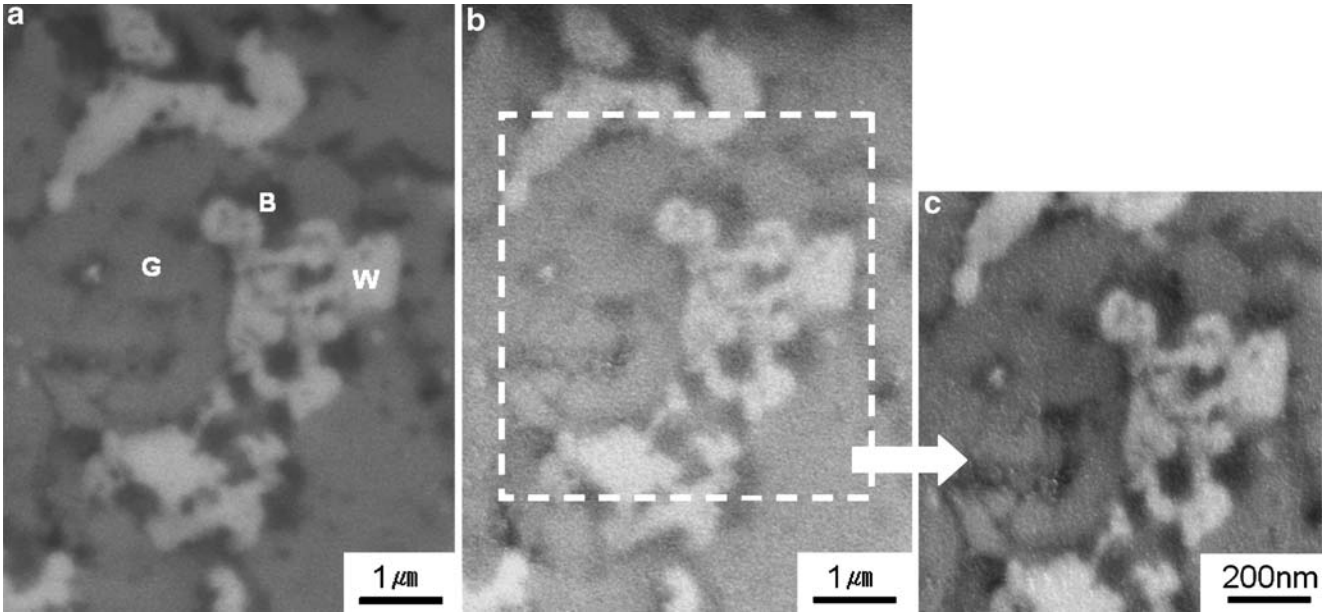

Fig. 5 Morphologies of C1 composites sintered at 850 °C: **a** Back scattering image, **b** SEM image, and **c** Magnified SEM image. *G* grey, *B* black, *W* white

sintered above 800 °C, the temperature coefficient of resonant frequency (τ_f) of C1 dramatically increases because of the crystal phases produced. However, the C1 composite sintered at 800 and 850°C has three different crystal phases (LaB_3O_6, $LaBO_3$–HT, and TiO_2). The crystal phase of TiO_2 is (+350~400) ppm/°C for τ_f according to the literature [21–23]. Based on the EDX, XRD, and network analysis results, as shown in Fig. 7, the unknown τ_f of crystal phases (LaB_3O_6 and $LaBO_3$–HT) was calculated with the volume fraction of crystal phase under the assumption that the determined temperature coefficient of resonant frequency might entail some errors that call for revision on the shape of phase and porosity.

To predict τ_f, it is suggested that the following empirical equation on the C1 composite sintered at 800 °C be applied: $(0.2 \times W) + (0.06 \times B(TiO_2 : + \ 350 \sim 400)) + (0.74 \times G) = 94$ and on the C1 composite sintered at 850 °C, $(0.32 \times W) + (0.12 \times B(TiO_2 : +350 \sim 400)) + (0.56 \times G) = 86$, where W is the temperature coefficient of the resonant frequency of the white region for $LaBO_3$–HT, G is the temperature coefficient of resonant frequency of the gray region for LaB_3O_6, and B is the temperature coefficient of resonant frequency of the black region for TiO_2. The τ_f value of $LaBO_3$–HT and LaB_3O_6 was found to be −63.75~−88.78 and +117~118.59 ppm/°C, respectively. Therefore, the results indicate that controlling the volume

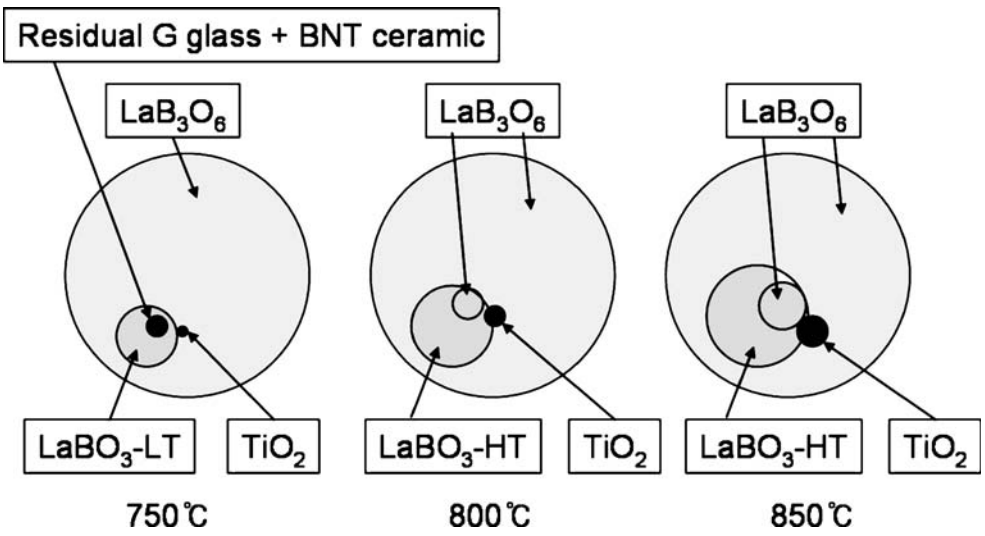

Fig. 6 Schematic diagram showing crystallization phenomena of a composite

Table 5 Microwave properties of C1 and C2 composite, G glass, and BNT ceramic.

Materials	Sintering temperature (°C)	f_0* (GHz)	ε_r	Q*f_0 (GHz)	τ_f (ppm/°C)
C1	750	7.8	13.5	6,146	39
	800	7.5	14.5	9,118	94
	850	7.5	14.2	9,852	86
C2	750	7.4	15.7	–[a]	–
	800	7.1	16.8	5,892	109
	850	7.2	16.6	–	–
G (LBT glass)	Room temperature	4.7	11.5	–	–
BNT Ceramic	1,280 (for 2.5 h)	4.2	90.7	6,141	6.24

[a] Not measured
*f_0: resonant frequency

of crystal phases with the temperature coefficient of the resonant frequency of the $LaBO_3$–HT and LaB_3O_6 might be an effective means to reduce the temperature coefficient of resonant frequency of the composites.

4 Conclusion

Using $20La_2O_3$–$60B_2O_3$–$20TiO_2$ glass, the composites of glass *(80 wt.%)* and BNT ceramic characterized by high sintering temperature (>1,220 °C) were sintered at a low temperature of <900 °C. The composite sintered at 850 °C achieved 90% relative density, 3% porosity, ≈15 dielectric constant, and ≈10,000 GHz quality factor (Q*f_0). The temperature coefficient of resonant frequency (τ_f), however, was quite high, 97 ppm/°C, which is attributed to the formation of TiO_2 crystal phase in the final crystal phases. The temperature coefficient of resonant frequency for the crystal phases of $LaBO_3$–HT and LaB_3O_6 was found using an empirical equation. Thus, a composite with suitable

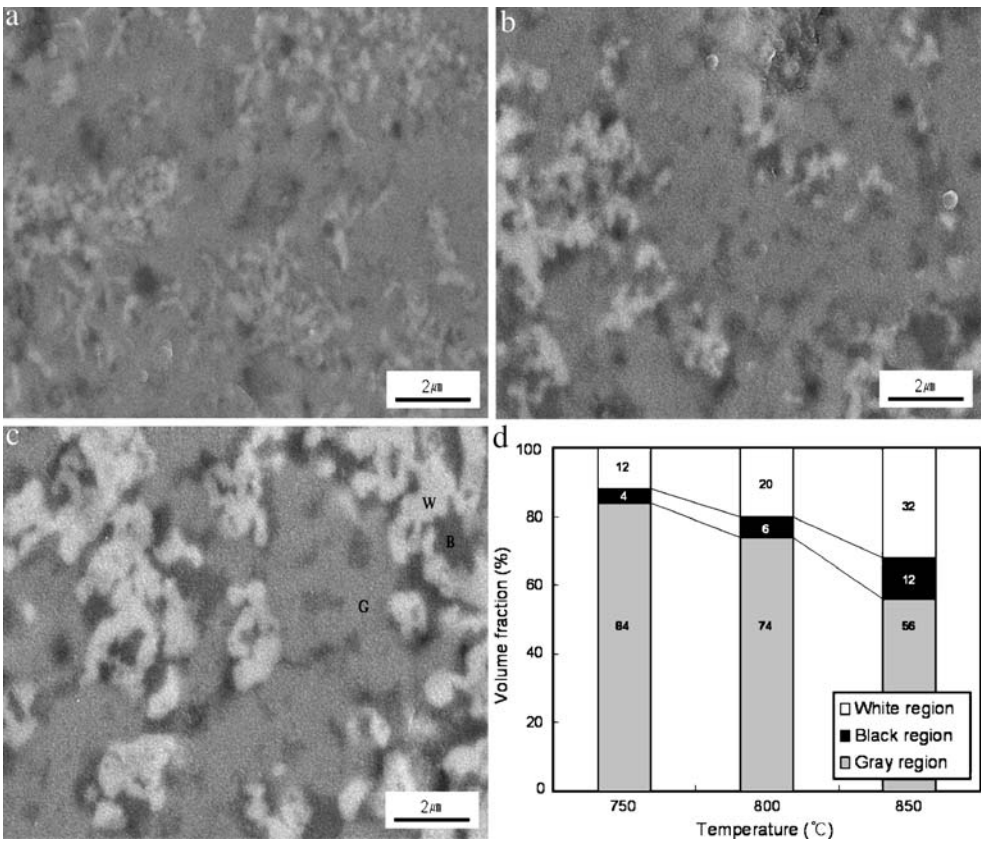

Fig. 7 Morphologies of C1 composites as a function of sintering temperature **a** 750 °C, **b** 800 °C, **c** 850 °C, and **d** volume fraction of region in the morphologies. *W* white, *B* black *G* grey region

additives for τ_f could feasibly be developed as a material for LTCC applications.

Acknowledgements This work was supported by grant No. 2003-042-D00101 of the Korea Research Foundation

References

1. R.R. Tummala, J. Am. Ceram. Soc. **74**, 895–908 (1991)
2. Y.J. Choi, J.H. Park, W.J. Ko, J.H. Park, S. Nahm, J.G. Park, J. Electroceramics **15**, 157–162 (2005)
3. L.C. Chang, B.S. Chiou, J. Electroceramics **15**, 75–81 (2005)
4. D.W. Kim, D.G. Lee, K.S. Hong, Mater. Res. Bull. **36**, 585–595 (2001)
5. C.C. Cheng, T.E. Hsieh, I.N. Lin, J. Euro. Ceram. Soc. **23**, 119–123 (2003)
6. J.M. Wu, H.L. Huang, J. Non-Cryst. Solids **260**, 116–124 (1999)
7. Y.J. Choi, J.H. Park, J.H. Park, J.G. Park, J. Mater. Lett. **58**, 3102–3106 (2004)
8. C.H. Lu, Y.H. Huang, Mat. Sci. Engi. **B98**, 33–37 (2003)
9. O. Dernovsek, A. Naeini, G. Preu, W. Wersing, M. Eberstein, W. Schiller, J. Euro. Soc. **21**, 1693–1697 (2001)
10. C.L. Lo, J.G. Duh, J. Am. Ceram. Soc. **85**, 2230–2235 (2002)
11. M. Eberstein, W. Schiller, O. Dernovsek, W. Wersing, Glastech. Ber. Glass Sci. Technol. **73 c1**, 370–373 (2000)
12. Y.J. Kim, S.J. Hwang, H.S. Kim, Mat. Sci. Forum **486–487**, 506–509 (2005)
13. B.H. Jung, S.J. Hwang, H.S. Kim, Mat. Sci. Forum **449–452**, 729–732 (2004)
14. B.H. Jung, S.J. Hwang, H.S. Kim, J. Euro. Ceram. Soc. **25**, 3187–3193 (2005)
15. C.R. Chang, J.H. Jean, J. Am. Ceram. Soc. **82**, 1725–1732 (1999)
16. B.W. Hakki, P.D. Coleman, IEEE Trans. Microwave Theor. Tech. **MTT-8**, 402–410 (1960)
17. W.E. Courtney, IEEE Trans. Microwave Theor. Tech. **MTT-18**, 476–485 (1970)
18. Y. Kovayashi, M. Katohy, IEEE Trans. Microwave Theor. Tech. **MTT-33**, 586–592 (1985)
19. M. Valant, D. Suvorov, Mat. Chemistry and Physics, **79**, 104–110 (2003)
20. T.P. Glesias, J.P. Fernandez, J. Chem. Thermodyn., **33**, 1375–1381 (2001)
21. S.X. Dai, R.F. Huang, D.L. Wilcox Sr., J. Am. Ceram. Soc. **85**, 828–832 (2002)
22. S.H. Yoon, D.W. Kim, S.Y. Cho, K.S. Hong, J. Euro. Ceram. Soc. **23**, 2549–2552 (2003)
23. C.T. Dervos, Ef. Thirios, J. Novacovich, P. Vassiliou, P. Skafidas, Mater. Lett. **58**, 1502–1507 (2004)